

Experimental diagnostics of multi-frequency quasiperiodic oscillations

N.V. Stankevich, A.P. Kuznetsov, E.S. Popova and E.P. Seleznev

June 30, 2016

*Kotel'nikov's Institute of Radio-Engineering and Electronics of RAS,
Saratov Branch,
Zelenaya 38, Saratov, 410019, Russian Federation.
Saratov State University
Astrakhanskaya, 83, 410012, Russian Federation.
Yuri Gagarin State Technical University of Saratov,
Politehnicheskaya 77, Saratov, 410054, Russian Federation.*

Abstract

We suggest a new technique of fold Poincaré section, allowing one to visualize an invariant curve of a multi-frequency invariant torus in a physical experiment. Details of the technique are presented, along with examples of its application to various experimental studies. Examples of how an invariant curve is visualized in double-, triple- and four-fold Poincaré sections are shown.

Keywords: quasiperiodic oscillations; invariant curve; fold Poincaré section.

1 INTRODUCTION

Quasiperiodic oscillations are widespread in science and engineering [1], [2], [3], [4]. One can find numerous examples in electronics, radio-engineering, biophysics, climatology, and astrophysics. Quasi-periodic oscillations can be

classified according to the number of independent incommensurable frequencies. The representation of quasi-periodic oscillations in phase space is an invariant torus. The dimension of a torus is equal to the number of incommensurable frequencies [5], a two-frequency torus being embedded into 3D space, three-frequency into 4D space etc. Spectra of the oscillations of such kind exhibit a complex structure and contain not only a set of basic frequencies, but also a set of their harmonics. The problems related to the generation of quasi-periodic oscillations, to their control by external driving, and to mutual synchronization of quasi-periodic oscillations are difficult, and an important advancement of the theoretical description of these phenomena was accomplished recently [5], [7], [6], [8], [9], [10], [11], [12], [13], [14], [15], [16]. One of the problems in studying multi-frequency quasi-periodic oscillations is their diagnostics. A traditional technique motivated from the physical point of view is the Fourier spectrum analysis. For two-frequency quasi-periodicity this technique is quite suitable, but for higher-dimensional oscillations Fourier spectrum becomes more complex due to a big number of harmonics. Another technique which arises from theory of dynamical chaos is the analysis of the spectrum of Lyapunov exponents. These exponents characterize the presence (absence) of the divergence of close phase trajectories [17]. Thus, for a system exhibiting chaotic oscillations, at least one Lyapunov exponent in the spectrum is positive. For quasi-periodic oscillations, several Lyapunov exponents become zero, and the number of zero Lyapunov exponents corresponds to the number of incommensurable frequencies. However, the process of calculating the complete spectrum of Lyapunov exponents with good accuracy takes a long time. Moreover, this technique is not applicable to experimental data since one can reliably detect only the largest Lyapunov exponent from a time realization.

Another technique is the construction of Poincaré section. For numerical simulations, it consists in finding points of intersection of a phase trajectory with some hyper-surface of the dimension less than the dimension of the phase space. An attractor corresponding to two-frequency quasi-periodic oscillations is a two-dimensional torus. Therefore, its intersection with a plane is an oval which is called an invariant curve.

Such diagnostics is very useful both for theoretical (or numerical) and experimental studies. However, an arousal of additional incommensurable frequencies blurs an invariant curve. In this case, the technique of the fold Poincaré section can be applied, which is the double Poincaré section in the simplest case. A three-frequency torus in the Poincaré section gives a set of

points forming an invariant curve (torus) in 3D space. This invariant curve can be intersected by a plane, and it gives an invariant curve in the double Poincaré section. We have to note that this set of points is discrete and does not coincide with an intersection plane. Therefore, in numerical calculations one needs to fix points inside some thin slice in such a case. Examples of using the double Poincaré section in theoretical studies can be found in Refs. [18], [19], [20]. As well, we have to note that the problems of multi-frequency oscillations are very difficult and a researcher should use different techniques which supplement each other [5], [7], [6], [8], [9], [10], [11], [12], [13], [14], [15], [16].

As for the experimental studies of multi-frequency quasi-periodicity, the Fourier spectrum analysis is typically used. We can mention Ref. [7] where the spectrum was simple enough and theoretical simulations of the system were realized. Combination of these approaches allowed one to identify new spectral components sufficiently easily. In Ref. [21], an algorithm allowing one to construct a parameter plane in an automatic regime and to distinguish between different kinds of dynamics including two-frequency and three-frequency quasi-periodicity was suggested on the basis of the Fourier spectrum analysis. In Ref. [22], the authors have constructed a phase map using an experimental time series. Quasi-periodic oscillations can be distinguished by this map. As for the technique of the fold Poincaré section, there is no experimental technique, where it is realized. We can mention only Refs. [23], [24], where mechanical systems vibrating in the external field were analyzed. In that paper the double Poincaré section was realized and plane of section was fixed by frequency of external action.

In the present paper the technique for diagnostics of multi-frequency quasi-periodic oscillations using the fold Poincaré sections is suggested and its applications to different electronic circuits are presented. The paper consists of three sections. In Sect. 2 the technique for construction of an invariant curve in the fold Poincaré section is described in detail for a generalized six-dimensional model with five frequencies, which can realize fourfold, triple and double Poincaré sections. In Sect.3 three applications of the technique to non-autonomous and autonomous coupled generators are given.

2 Technique for visualization of invariant curve in fold Poincaré section

The main idea of the construction of Poincaré section is to trace the values of several dynamical variables at a certain time instant. The Poincaré section is most easily realized in non-autonomous systems, as there is a time scale corresponding to the period of an external force. In this case one can use the so-called stroboscopic section, in this case section plane should be chosen through period of external action. In an experiment it is realized in the following way. A signal of an external force from a standard generator of harmonic oscillations is applied to an autonomous system. The same signal is applied to an external trigger input of a pulse generator. Dynamical variables of the autonomous system are fed to inputs X and Y of an oscilloscope working in the X-Y regime. On the screen of the oscilloscope a projection of phase portrait on the plane (X, Y) is formed. Short pulses from the output of a pulse generator are fed to input of external lighting of image of oscilloscope. Varying brightness of the beam of oscilloscope, one can observe a projection of a phase portrait on the screen of oscilloscope and its stroboscopic section. An attractor in a stroboscopic section is formed in that way on the screen of the oscilloscope. Such a technique for visualization of an invariant curve was realized in Refs. [23], [24], [25].

In the case of a two-dimensional torus in the Poincaré section, one can observe an invariant curve. It will change at varying of controlling parameters and one can talk about evolution of quasi-periodic oscillations. If the curve transforms into a discrete set of points, then we can talk about synchronization on a torus. If a sharp curve appears, one can suggest the presence of a strange non-chaotic attractor [26], [27], [28]. If curve is blurred, then it can represent a transformation to three-frequency torus or transition to chaos.

If number of frequency components increases we have to realize double, triple or more Poincaré section in the system under study, in order to visualize invariant curve. For non-autonomous system it means that number of external forces is increased. For visualization of invariant curve in fold Poincaré section one should find time instant when periods of different external forces are coincident. We should notice that the probability of coincidence of pulses in the scheme is small enough, and it decreases with increasing of fold of section. As the result, the time intervals between pulses occurring in the scheme output become large. And one can not see fold Poincaré section on

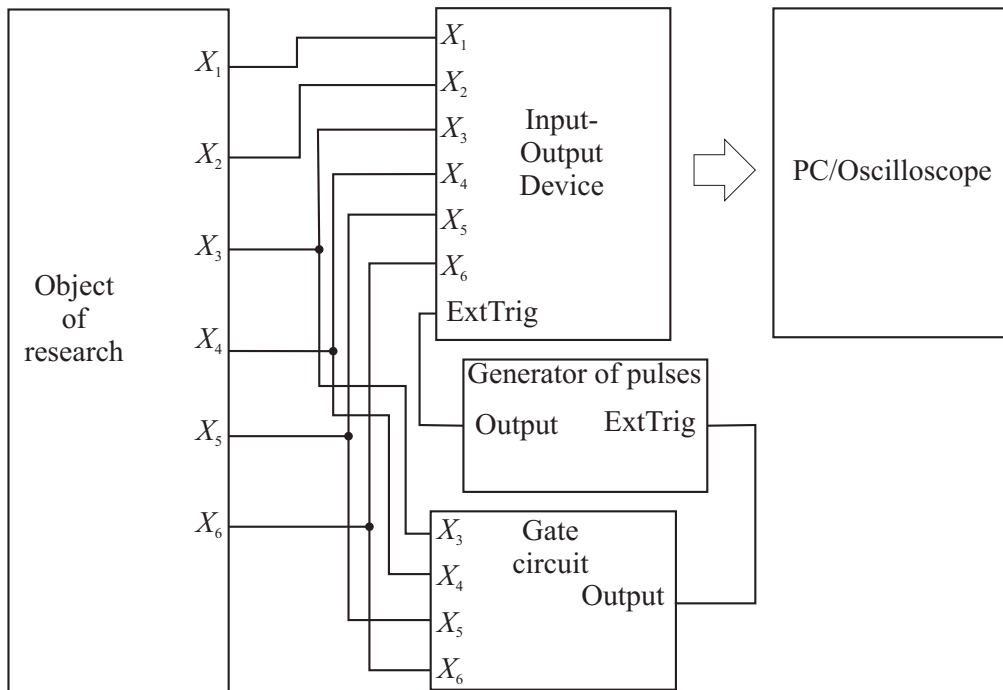


Figure 1: Principle scheme for realization of four-fold Poincaré section

the screen of oscilloscope. Then one can use a personal computer (PC) with input-output analog signals. In our experiment we use PC with IO analog signals NI USB-6211.

The situation is more complicated in the case of studying an autonomous system. For constructing of one-dimensional Poincaré section one should choose fixed value of dynamical variable. When dynamical variable reaches out this value, then stroboscopic pulse is formed and light on certain point of phase portrait on the screen of oscilloscope (or it can be written to PC). If we talk about multi-dimensional Poincaré section, then we have to determine the moment, when several dynamical variables reach out some fixed values. In Fig. 1 principle scheme allowing to realize four-fold Poincaré section is shown (in Appendix A1 one can find values of the all elements of the gate circuit). The minimal dimension of phase space of such system has to be six, and maximal number of frequencies equals to five. Dynamical variables $X_1, X_2, X_3, X_4, X_5, X_6$ are applied to the input of input-output device for recording to the PC, and variables X_3, X_4, X_5, X_6 are applied to the inputs

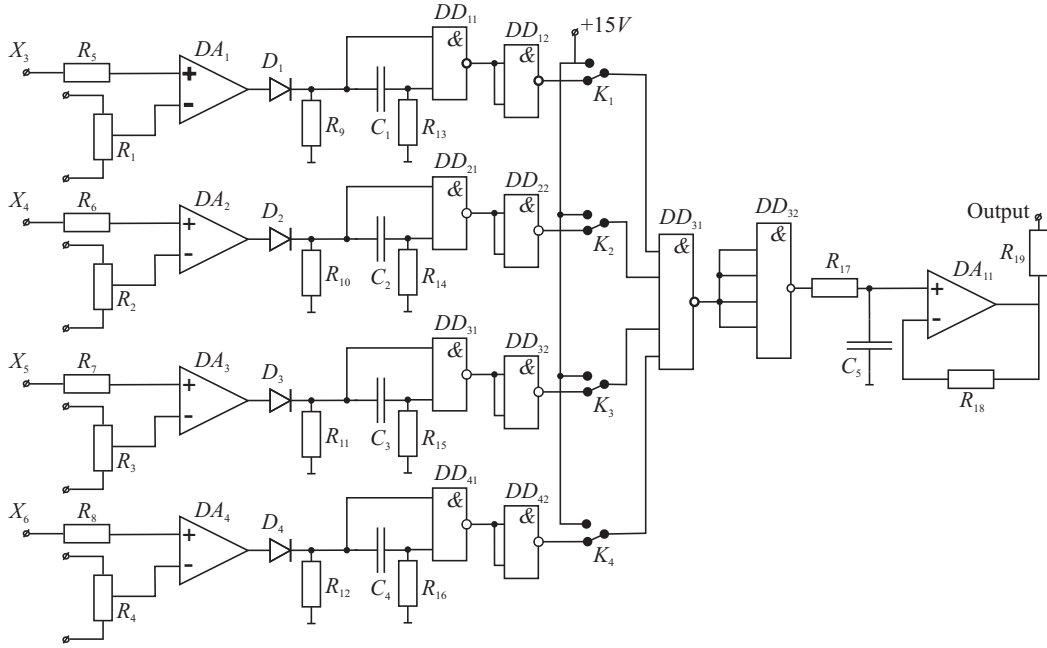


Figure 2: Scheme of the gate circuit

of gate circuit, which formed controlling pulses for recording of date. In Fig. 2 structure of gate circuit, providing realization of four-fold Poincaré section is shown. Gate circuit represents the set of comparators of voltage (DA_1 - DA_4), in inputs of which go the corresponding dynamical variables X_3 , X_4 , X_5 , X_6 . Potentiometers R_1 - R_4 determine operational thresholds. Until value of dynamical variable is less than the threshold value, voltage on the output of comparator is equal to $-E_{pit}$. At the moment when dynamical variable reaches out threshold value, then comparator switches to state when voltage on the output of comparator is equal to $+E_{pit}$. Positive drops of voltage, corresponding to reach out of dynamical variable determined by potentiometers R_1 - R_4 values, are applied to inputs of formers of short pulses realized on the logic elements DD_{11} - DD_{42} with chains $R_{13}C_1$ - $R_{16}C_4$. Consequently the part of scheme, including elements DA_1 - DA_4 , R_1 - R_4 , DD_{11} - DD_{41} , $R_{13}C_1$ - $R_{16}C_4$ and DD_{12} - DD_{42} provides formation of short pulses at the moment, when dynamical variables reach out threshold values. In experiment, pulse width was the same for different variables and equal to $1/100$ of the least period of oscillations of self-generators. Definition of the moment, when these events occur simultaneously is provided by logical gate DD_{31} and reverser DD_{32} .

At the moment when all dynamical variables reach out threshold values to all inputs DD_{31} rectangle pulses (logical units) are applied, consequently in output DD_{31} one pulse occurs. Further, the pulse output from the gate circuit is applied to the input of the external trigger standard pulses generator, on the output of which rectangle pulse with parameters necessary to run input-output devices is formed. At the moment of arrival of the pulse input to the external trigger input and output devices the instantaneous values of dynamical variables are read. These variables are transmitted to the PC, where invariant curve is visualized. By means of a time shift between output and trigger pulses, one can displace the cross sections of the attractor in the projection and choose more clear option.

Using switches K_1-K_4 in gate circuit, we can change fold of Poincaré section from single to four-fold and also we can observe sections by different variables. This circuit allows one to observe invariant curve in four-fold Poincaré section for five-frequency torus. Visualization of invariant curve was realized in PC with using software LabView. In LabView we can limit parameter *Time*, which is responding for time of producing and processing of the data. The gate circuit can be extended for system of any dimension and any number of frequencies. But one should understand that increasing of section fold entails increasing of time observation and getting of experimental data. In the experiment for constructing four-fold Poincaré we set parameter *Time* equal 20 minutes.

3 Examples of applying the technique of fold Poincaré section for different kind systems

3.1 Non-autonomous nonlinear oscillator

From the beginning we consider the simplest case, when an object under study is a non-autonomous system. We consider nonlinear oscillatory RLD-circuit excited by the signal representing the sum of three harmonic components $A_1 \sin(\omega_1 t)$, $A_2 \sin(\omega_2 t)$ and $A_3 \sin(\omega_3 t)$. Accordingly, we deal with dynamical system with five-dimensional phase space and three independent frequencies. The circuit scheme is shown in Fig. 3. In Appendix A2 one can find all parameters of elements. Values of frequencies of external force were chosen in the following way: ω_1 was close to linear resonance frequency of oscillatory circuit and equals 51 kHz, $\omega_2 = k_2 \omega_1$, $\omega_3 = k_3 \omega_1$, where k_2 and k_3

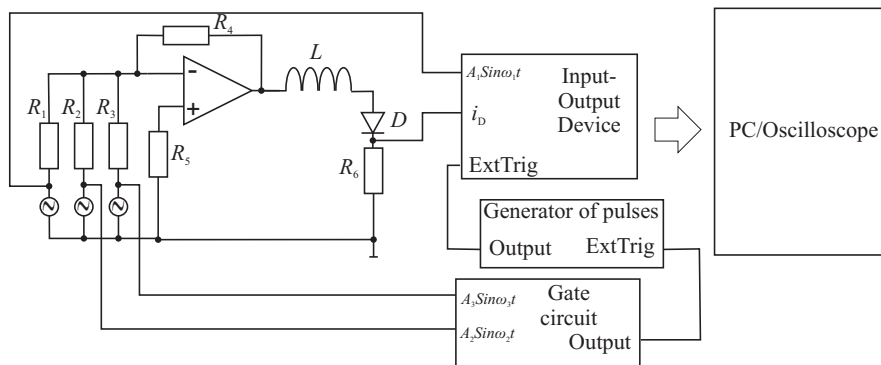


Figure 3: Scheme of electronic circuit of the RLD-contour

are irrational numbers, which represent solutions of minimal polynomial of second and third degree: $k_2 = \frac{\sqrt{5}-1}{2}$, $k_3 = 1.324718$ [29]. At $A_1 \neq 0$, $A_2 \neq 0$ and $A_3 \neq 0$ three-frequency torus can be realized in the studying system. In order to visualize invariant curve of three-frequency torus we have to realize double Poincaré section. As the section variable we use second and third frequencies ($\omega_2 t$ and $\omega_3 t$ correspondingly). Character of oscillations was analyzed by projection of phase portrait on plane $(A_1 \sin(\omega_1 t), i_D)$, where i_D is intensity of diode current and $A_1 \sin(\omega_1 t)$ represents phase of corresponding harmonic of external force. In Fig. 4 one can find examples of attractors in double Poincaré section in projection on this plane. We use projection on this plane due to the fact that this plane shows the dependence of behavior of dynamical variable on the phase of external action. If we observe smooth invariant curve then we can talk about stability of dynamics. Appearance of breaks and blurring on phase portrait indicates local instability and in general the presence of phase-dependent dynamics.

A phase portrait in Fig. 4a corresponds to smooth three-frequency torus. Some blurring of attractor in Poincaré section is caused by the finite time interval of coincidence, which is limited by twice length of the pulses in the gate circuit. In our experiment this interval was limited by $0.5 \mu Sec$. Phase portrait in Fig. 4b corresponds to double three-frequency torus. Dynamical regime in Fig. 4c corresponds to quadruple three-frequency torus. In double Poincaré section it can be four close invariant curves or it can be embedded four times invariant curve. In Fig. 4d chaotic oscillations occurring via torus break down are illustrated.

In Figs. 4e-h, Fourier spectra are shown for three-frequency quasi-periodic

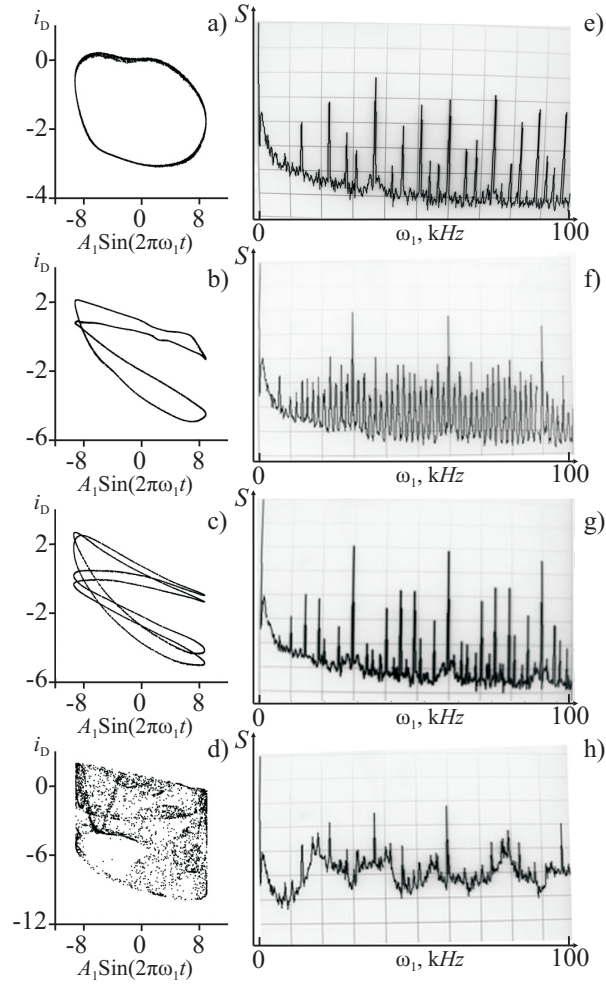


Figure 4: Examples of visualization of invariant curve in double Poincaré section by hyper-surface $A_2 \sin(\omega_2 t)=0$, $A_3 \sin(\omega_3 t)=0$ and Fourier spectra for different values of A_2 and A_3 : a), e) $A_2=0.19$ V, $A_3=0.18$ V; b), f) $A_2=0.18$ V, $A_3=0.57$ V; c), g) $A_2=0.03$ V, $A_3=0.83$ V; d), h) $A_2=0.3$ V, $A_3=0.75$ V.

torus, for doubled torus and for chaotic oscillations. As one can see, it is sufficiently difficult to distinguish this different kind of dynamics by spectrum, but fold Poincaré section allows one to distinguish it with a good accuracy.

3.2 Two coupled generators of quasi-periodic oscillations

Now we apply the technique of visualization of invariant curve in fold Poincaré section for autonomous system (without external action). We consider two coupled generators of quasi-periodic oscillations. In Refs. [30], [31] the models of generators of quasi-periodic oscillations with minimal dimension of phase space ($N = 3$) was suggested. In [32] an electronic circuit implementing generator of such kind was realized and for this generator two-frequency quasi-periodic oscillations were observed.

In Fig. 5a the scheme of electronic circuit of generator of quasi-periodic oscillations is shown. The generator represents classical oscillator with inductive feedback based on the two gate field effect transistor. It includes active oscillator consisting of inductor L_1 , capacitor C_1 , nonlinear elements represented by back-to-parallel linked semiconductors diodes (D_1 - D_4) and of field effect transistor T_1 , and control circuit. The control circuit consists of multiplier DA_4 and integrator DA_3 . The potential outputted of integrator U_{1g2} is applied at the second gate of field effect transistor. The control parameters of this generator are defined by the resistances R_8 and R_{12} , which regulate integration time of the amplifier DA_3 and amplitude of self-oscillating of active oscillator by way of changing of the additional voltage U_0 .

We consider two coupled generators. This generators were identical. Values of the elements on the Fig.5 a are presented in Appendix A3. In Fig. 5b one can see function diagram of experimental circuit, including two generators, gate circuit, input-output devices and PC. The dynamical variables are voltage of each oscillate contours U_1 , U_2 and their derivative \dot{U}_1 , \dot{U}_2 , and also voltage on the second gate of the field effect transistors U_{1g2} , U_{2g2} . Coupling between oscillators is resistive, realized by resistor R_C . Thus, the system has six-dimensional phase space and four independent frequencies. At small coupling the four-frequency quasi-periodic oscillations are possible. In order to visualize invariant curve of this torus it is necessary to realize triple Poincaré section.

The feature of the present system is that each oscillator has three dynamical

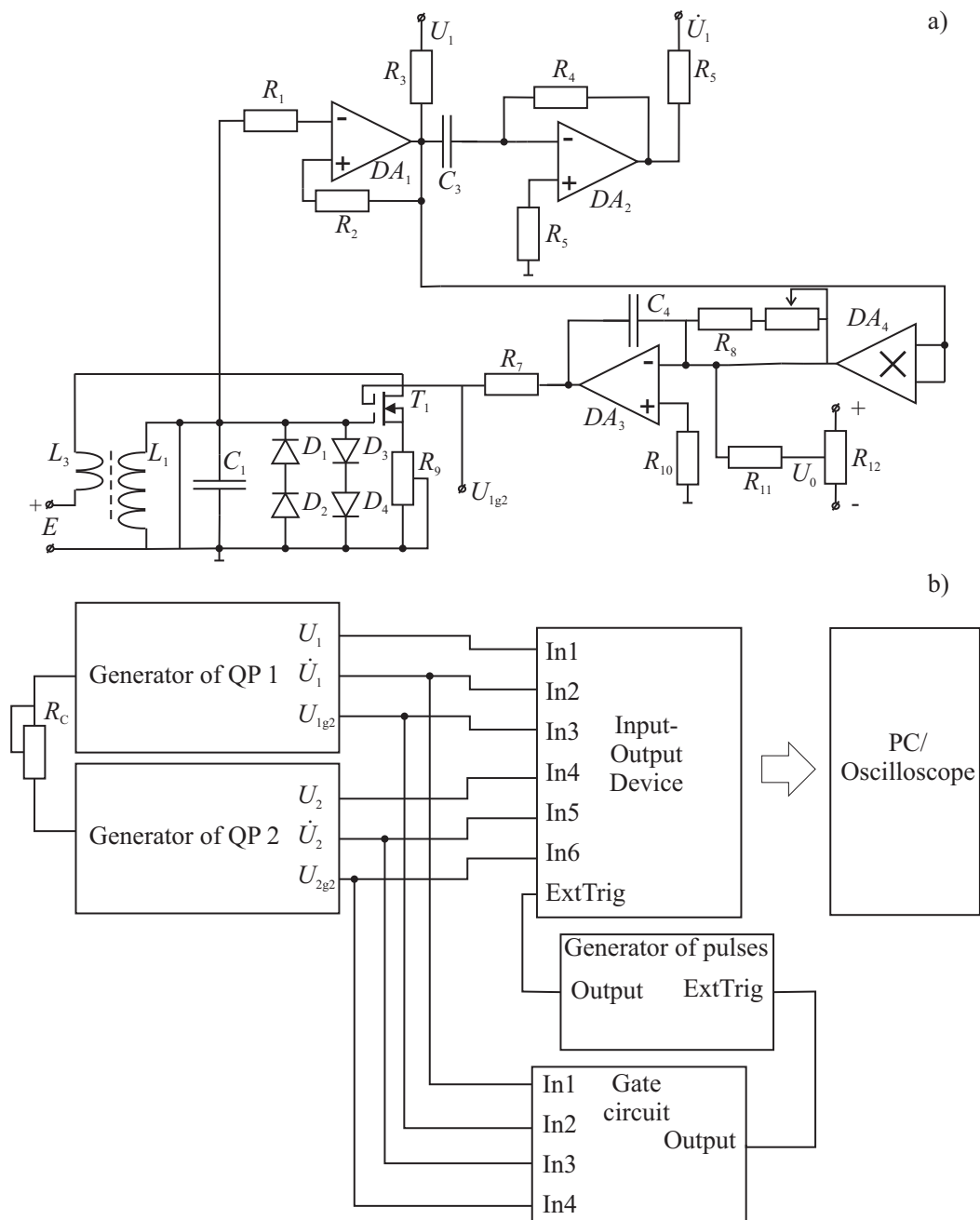


Figure 5: a) Scheme of electronic circuit of the single generator of quasi-periodic oscillations; b) Function diagram of circuit of two coupled oscillators for realization of fold Poincaré section.

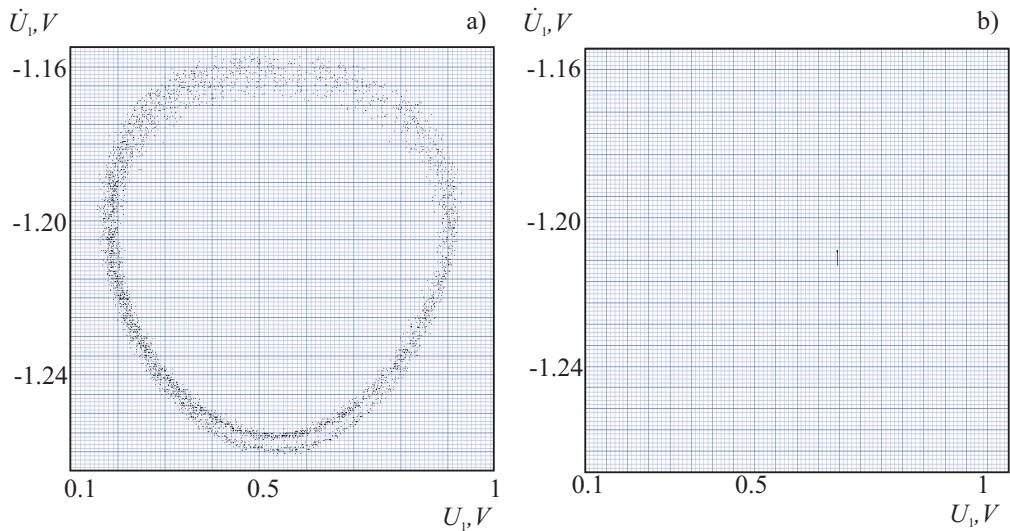


Figure 6: Two-dimensional projections of phase portraits of the system of two coupled generators of quasi-periodic oscillations; a) in the single Poincaré section by hyper-surface $U_2 = 0$; b) in the double Poincaré section by hyper-surface $U_2 = 0, \dot{U}_2 = 0$.

ical variables, and two of them U_1 and \dot{U}_1 are fast enough, and the third U_{1g2} corresponds to relaxation oscillations and it is slow enough. At one period of relaxation oscillations there are 60 oscillations of self-generators. In order to visualize invariant curve of four-frequency torus we should realize triple Poincaré section. If we realize Poincaré section by derivative of one of variables, then dynamics of these variables will be limited. It is more reasonable to make cross-section by variables of one coupled subsystem and to observe for variables of another subsystem. In our case it has to be cross-section by all variables of the one generator. But in this case we have problem connected with relaxation character of one variable on the second gate of field effect transistor, since this variable is very slow and we cannot visualize invariant curve of four-frequency torus in triple Poincaré section.

However, we can choose parameters of generators and visualize invariant curve of two-frequency oscillations corresponding to the regime of phase synchronization of quasi-periodic oscillations [6], [32] and realize double and triple Poincaré section. Figure 6 shows phase portrait in Poincaré section on plane (U_1, \dot{U}_1) in single Poincaré section (Fig. 6a) and in double Poincaré section (Fig. 6b). As one can see, invariant curve in this case is vanishing,

but in double section there is a fixed point. Consequently, if one realize k -fold Poincaré section for a system with k -frequency torus, then one will get fixed point in the Poincaré section. Such approach can be applied for detecting bifurcation lines on the parameter planes for systems with multi-frequency quasi-periodic oscillations.

3.3 Five coupled van der Pol oscillators

In connection with the problem occurring at visualization of four-frequency torus in six-dimensional system, we consider the system of five coupled oscillators. Each oscillator is characterized by two phase variables and one frequency of own oscillations. Therefore, we deal with ten-dimensional system and with five incommensurable frequencies. In Fig. 7c the functional diagram of electronic circuit is presented. In Fig. 7a one can see the scheme of electronic circuit of one generator of van der Pol type. Each generator consists of an oscillatory circuit formed by inductors L_1 and capacitors C_i (i is number of oscillator), and of nonlinear elements represented by back-to-parallel linked semiconductor diodes (D_1 - D_2). In Fig. 7b the voltage-current characteristic of the combined resistance composed of a linear negative conductance realized by an operational amplifier and a bidirectionally connected diodes is shown. Oscillators are differ only by frequencies. All another parameters is identical for each oscillator and can be find in Appendix A4. Frequency mismatch between frequencies of oscillators was realized by different capacity of capacitors C_i . Excitation of the self-oscillations occurs due to the negative resistance blocks (R_1) assembled on the operational amplifiers (DA_{11}). R_2 and R_3 represent negative feedback circuit of operational amplifier DA_{11} . Varying resistance of the resistor R_2 we can change coefficient of amplifier. The dynamical variables are voltage outputs from operational amplifiers (DA_{11}), and its derivative, formed by derivative amplifiers (DA_{12}). The coupling between the generators is provided by variable resistor $R_{i,i+1}$, $i = (1 \div 5)$, connecting identical points of the two circuits, and we consider the system with ring coupling, $R_{56}=R_{51}$ (Fig. 7c). The strength of coupling is inversely proportional to the resistor. Dynamical variables X, \dot{X}, Y, Z, W, V input to IO device and variables $\dot{Y}, \dot{Z}, \dot{W}, \dot{V}$ input to gate circuit.

At small coupling the system demonstrates five-frequency quasi-periodic oscillations. With increasing of coupling the one of the frequencies will be locked and we can observe transition from five-frequency torus to the four-frequency torus and the three-frequency torus. In order to distinguish quasi-

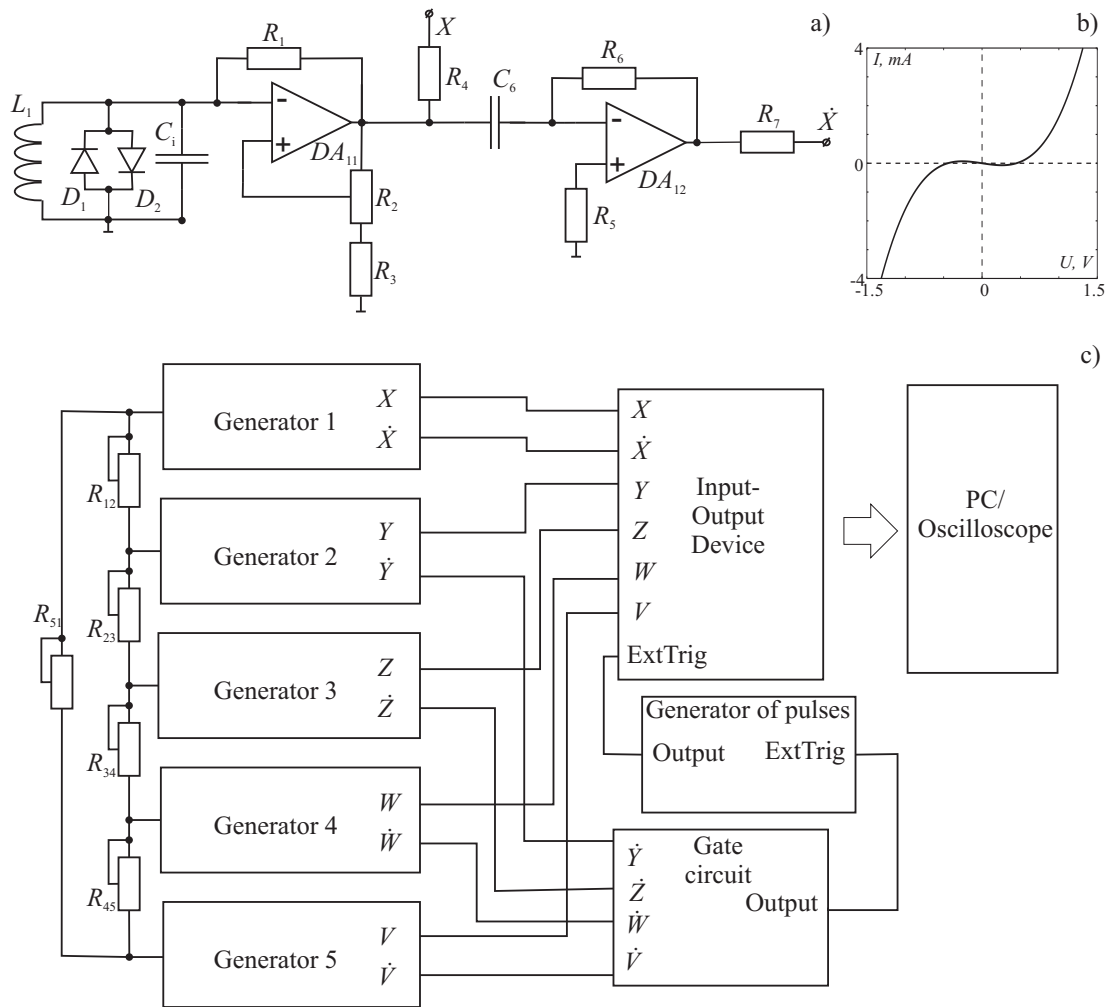


Figure 7: a) Scheme of electronic circuit of the single generator of van der Pol type; b) Voltage-current characteristic of the combined resistance composed of a linear negative conductance realized by operational amplifier and nonlinear element of the single generator of van der Pol type; c) Function diagram of circuit of five coupled in ring oscillators for realization of fold Poincaré section.

periodic oscillations with different number of frequency components we apply technique of visualization of fold Poincaré section. For visualization of invariant curve of five-frequency quasi-periodic oscillation we should realize four-fold Poincaré section. In order to escape situation which occurred in the case of two coupled generators of quasi-periodic oscillations we will analyze dynamical variables of the one of oscillators (X, \dot{X}) and one of variables of another oscillators (Y, Z, W, V), and realize Poincaré sections by derivatives of another variables ($\dot{Y}, \dot{Z}, \dot{W}, \dot{V}$). In Fig. 7c one can see function diagram of experiment circuit. Using switches K_1-K_4 in gate circuit, we can change fold of Poincaré section from single to four-fold.

In Figs. 8-10, different examples of the phase portraits in fold Poincaré sections are shown for system of five coupled oscillators.

In Fig. 8, fold Poincaré sections of phase portrait of five-frequency quasi-periodic torus are shown. Figure 8a represents original two-dimensional projection of phase portrait on the dynamical variables of the first generator (X, \dot{X}), Figs. 8b-e represent single (by section hyper surface $\dot{Y} = 0$), double (by section hyper surface $\dot{Y} = 0, \dot{Z} = 0$), triple (by section hyper surface $\dot{Y} = 0, \dot{Z} = 0, \dot{V} = 0$) and four-fold (by section hyper surface $\dot{Y} = 0, \dot{Z} = 0, \dot{V} = 0, \dot{W} = 0$) Poincaré section in projection on the same plane. In Fig. 8e one can see invariant curve and identify five-frequency quasi-periodic regime.

In Fig. 9, fold Poincaré sections of phase portrait of four-frequency quasi-periodic torus are shown. Figure 9a corresponds to the single Poincaré section, and Figs. 9b and c to the double and triple sections. In the triple Poincaré sections one can observe clear invariant curve.

For the system of five coupled oscillators in experiment bifurcation of doubling of three-frequency torus at varying of control parameters was observed. In Fig. 10, transformation of phase portraits corresponding to this bifurcation is shown. In Fig. 10, phase portraits are indicated by red color (colored on-line) and invariant curves in double Poincaré section are indicated by blue color. Figure 10a corresponds to the situation before bifurcation and Fig. 10b corresponds to the situation after bifurcation. As one can see, invariant curve very-well demonstrates such kind of transformation.

4 Conclusion

Thus, the technique of visualization of invariant curve in the fold Poincaré section is effective technique for diagnostic and distinguishing multi-frequency

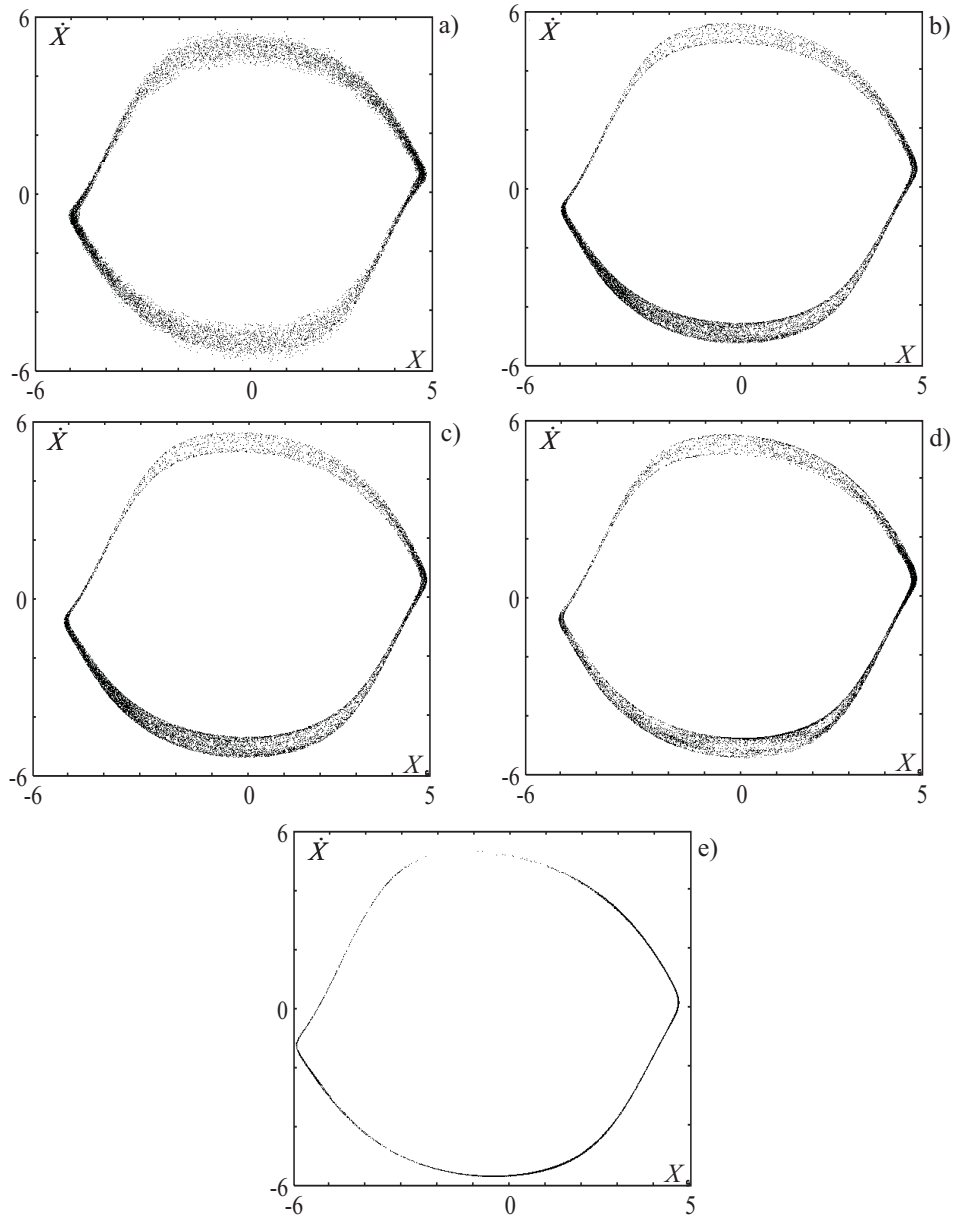


Figure 8: Phase portraits of five-frequency torus of five coupled oscillators
a) without section; b) in the single Poincaré section by hyper-surface $\dot{Y} = 0$;
c) in the double Poincaré section by hyper-surface $\dot{Y} = 0, \dot{Z} = 0$; d) in the
triple Poincaré section by hyper-surface $\dot{Y} = 0, \dot{Z} = 0, \dot{W} = 0$; e) in the
four-fold Poincaré section by hyper-surface $\dot{Y} = 0, \dot{Z} = 0, \dot{W} = 0, \dot{V} = 0$.

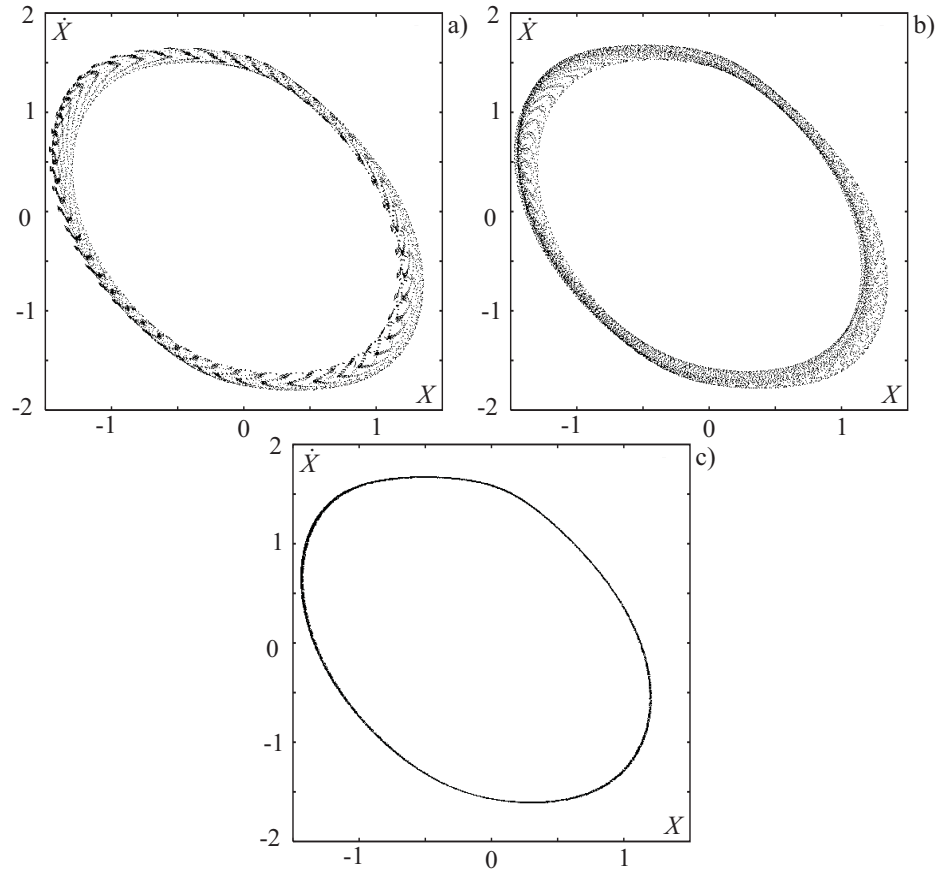


Figure 9: Phase portraits of four-frequency torus of five coupled oscillators
a) in the single Poincaré section by hyper-surface $\dot{V} = 0$; b) in the double Poincaré section by hyper-surface $\dot{W} = 0, \dot{V} = 0$; c) in the triple Poincaré section by hyper-surface $\dot{Z} = 0, \dot{W} = 0, \dot{V} = 0$.

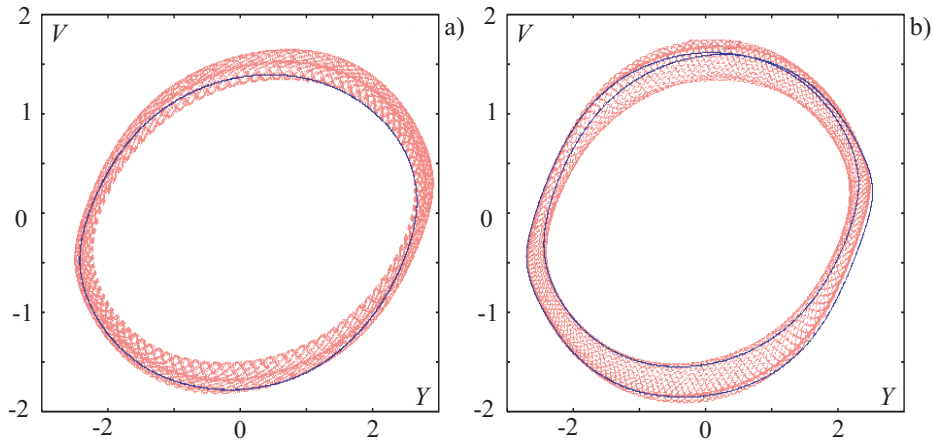


Figure 10: Doubling of three-frequency tori in the system of five coupled generators of van der Pol type. Red color corresponds to phase portraits in projection (X, \dot{X}) , blue color corresponds to phase portraits in double Poincaré section by hyper-surface $\dot{Y} = 0, \dot{V} = 0$.

quasi-periodic oscillations. The technique has good relevance for studying non-autonomous systems. In case of autonomous systems, the technique can be applied to systems satisfying the condition of $N = 2F$, where N is dimension of phase space of the system and F is the number of frequencies of the system. The condition allows one to realize procedure of fold Poincaré section correctly.

In the present paper we have shown the examples of four-fold Poincaré sections, but such technique can be generalized to any number of frequencies.

This research was supported by the Grant of Russian Scientific Foundation (Project 14-12-00291).

5 Appendix A

Parameter values of elements of electronic circuits, which were used in the experiments.

A1. Gate circuit (Fig.2)

$$R_1=10 \text{ k}\Omega, R_2=10 \text{ k}\Omega, R_3=10 \text{ k}\Omega, R_4=10 \text{ k}\Omega,$$

$$R_5=10 \text{ k}\Omega, R_6=10 \text{ k}\Omega, R_7=10 \text{ k}\Omega, R_8=10 \text{ k}\Omega,$$

$$D_1-D_4 \text{ are semiconductors diodes KD522,}$$

$$R_9=10 \text{ k}\Omega, R_{10}=10 \text{ k}\Omega, R_{11}=10 \text{ k}\Omega, R_{12}=10 \text{ k}\Omega,$$

$C_1=12$ pF, $C_2=12$ pF, $C_3=12$ pF, $C_4=12$ pF,
 $R_{13}=100$ k Ω , $R_{14}=100$ k Ω , $R_{15}=100$ k Ω , $R_{16}=100$ k Ω ,
 $C=100$ pF, $R_{17}=100$ k Ω , $R_{18}=10$ k Ω , $R_{19}=1$ k Ω .

A2. Non-autonomous RLD-contour (Fig.3)

$R_1=10$ k Ω , $R_2=10$ k Ω , $R_3=10$ k Ω , $R_4=10$ k Ω ,
 $L=30$ mH, $R_6=50$ Ω ,

D is semiconductors diode KD522.

A3. Generator of quasi-periodic oscillations (Fig. 5a)

$R_1=10$ k Ω , $R_2=10$ k Ω , $R_3=1$ k Ω , $R_4=10$ k Ω ,
 $R_5=1$ k Ω , $R_6=620$ Ω , $R_7=1$ k Ω , $R_8=100$ k Ω ,
 $L_1=100$ μ H, $C_1=510$ nF, $C_3=1000$ nF, $C_4=22$ nF,
 $R_9=200$ Ω , $R_{10}=620$ Ω , $R_{11}=10$ k Ω , $R_{12}=10$ k Ω ,
 D_1 - D_4 are semiconductors diodes KD522,

T_1 is field-effect transistor.

A4. Generator of van der Pol type (Fig. 7a)

$L_1=250$ mH,
 $C_1=1000$ pF, $C_2=680$ pF, $C_3=510$ pF, $C_4=330$ pF, $C_5=220$ pF,
 $R_1=62$ k Ω , $R_2=20$ k Ω , $R_3=1$ k Ω , $R_4=1$ k Ω ,
 $C_6=1000$ pF, $R_5=620$ Ω , $R_6=10$ k Ω , $R_7=1$ k Ω .

References

- [1] Pikovsky A., Rosenblum M., Kurths J. Synchronization: A Universal Concept in Nonlinear Science. Cambridge, England: Cambridge University Press; 2001.
- [2] Landa P.S. Nonlinear oscillations and waves in dynamical systems. Springer Science & Business Media; 2013. Vol.503.
- [3] Baesens C., Guckenheimer J., Kim S., MacKay R.S. Three coupled oscillators: mode locking, global bifurcations and toroidal chaos // Physica D. 1991. Vol. 49. PP. 387-475.
- [4] Hopf E. A mathematical example displaying features of turbulence // Communications on Pure and Applied Mathematics. 1948. Vol.1. PP. 303-322.
- [5] Anishchenko V.S. Dynamical Chaos in Physical Systems. Teubner, Leipzig; 1985.

- [6] Anishchenko V., Nikolaev S., Kurths J. Winding number locking on a two-dimensional torus: Synchronization of quasiperiodic motions // *Phys. Rev. E*. 2006. Vol.73. P. 056202.
- [7] Anishchenko V. S., Astakhov S. V., Vadivasova T. E., Feoktistov A. V. Numerical and experimental study of external synchronization of two-frequency oscillations // *Nelineinaya Dinamika*. 2009. Vol. 5. No. 2. PP. 237-252. (In Russia)
- [8] Emelianova Yu.P., Kuznetsov A.P., Sataev I.R., Turukina L.V. Synchronization and multi-frequency oscillations in the low-dimensional chain of the self-oscillators // *Physica D*. 2013. Vol. 244. No 1. PP. 3649.
- [9] Kuznetsov A.P., Kuznetsov S.P., Sataev I.R., Turukina L.V. About LandauHopf scenario in a system of coupled self-oscillators // *Physics Letters A*. 2013. Vol. 377. PP. 32913295.
- [10] Stankevich N.V., Kurths J., Kuznetsov A.P. Forced synchronization of quasiperiodic oscillations // *Communications in Nonlinear Science and Numerical Simulation*. 2015. Vol.20. PP. 316-323.
- [11] Inaba N., Kamiyama K., Kousaka T., Endo T. Numerical and experimental observation of Arnold resonance webs in an electrical circuit // *Physica D: Nonlinear Phenomena*. 2015. Vol. 311. PP. 17-24.
- [12] Sekikawa M., Inaba N., Kamiyama K., Aihara K. Three-dimensional tori and Arnold tongues // *Chaos: An Interdisciplinary Journal of Nonlinear Science*. 2014. Vol. 24. No.1. P. 013137.
- [13] Hidaka S., Inaba N., Sekikawa M., Endo T. Bifurcation analysis of four-frequency quasi-periodic oscillations in a three-coupled delayed logistic map // *Physics Letters A*. 2015. Vol. 379. No. 7. PP. 664-668.
- [14] Rosenblum M. and Pikovsky A. Two types of quasiperiodic partial synchrony in oscillator ensembles // *Physical Review E*. 2015. Vol. 92. P. 012919.
- [15] Zhusubaliyev Zh.T., Mosekilde E., Pavlova E.V. Multistability and torus reconstruction in a DC/DC converter with multilevel control. // *IEEE Trans. Ind. Inform.* 2013, Vol. 9. PP. 1937-1946.

- [16] Zhusubaliyev Z.T., Mosekilde E., Andriyanov A.I., Shein V.V. Phase synchronized quasiperiodicity in power electronic inverter systems // *Physica D: Nonlinear Phenomena*. 2014. Vol. 268. PP. 14-24.
- [17] Broer H., Simò C., Vitolo R. Quasi-periodic bifurcations of invariant circles in low-dimensional dissipative dynamical systems // *Regular and Chaotic Dynamics*. 2011. Vol. 16. No. 1-2. PP. 154-184.
- [18] Postnov D.E., Balanov A.G., Sosnovtseva O.V. Transition to synchronized chaos via suppression of the natural dynamics // *Physics Letters A*. 2001. Vol. 283. Issues 3-4. PP. 195-200.
- [19] Camparo J.C., Frueholz R.P. Attractor geometry of a quasiperiodically perturbed, two-level atom // *Phys. Rev. A*. 1991. Vol. 43. No.1. PP. 338-345.
- [20] Maistrenko V., Vasylenko A., Maistrenko Yu., and Mosekilde E. Phase chaos in the discrete Kuramoto model // *International Journal of Bifurcation and Chaos*. 2010. Vol. 20. Issue 6. P.1811-1823.
- [21] Linsay P.S., Cumming A.W. Three-frequency quasiperiodicity, phase locking and the onset of chaos // 1989. *Physica D*. Vol. 40. PP. 196-217.
- [22] Ashwin P., Swift J.W. Unfolding the torus: oscillator geometry from time delays // *Journal of Nonlinear Science*. 1993. Vol.3. PP. 459-475.
- [23] Moon F.C., Holmes W.T. Double Poincaré sections of a quasiperiodically forced, chaotic attractor // *Physics Letters A*. 1985. Vol. 111. Issue 4. PP. 157-160.
- [24] Virgin L.N., Nichols J.M. An Experimental Nonlinear Oscillator Subject to Two-frequency Excitation // *Proceeding of IMAC-XXV: Conference & Exposition on Structural Dynamics*. <http://sem-proceedings.com/25i/sem.org-IMAC-XXV-s33p02-An-Experimental-Nonlinear-Oscillator-Subject-Two-frequency-Excitation.pdf>
- [25] Kuznetsov A.P., Seleznev E.P., Stankevich N.V. Nonautonomous dynamics of coupled van der Pol oscillators in the regime of amplitude death // *Communications in Nonlinear Science and Numerical Simulation*. 2012. Vol. 17. No. 9. PP. 3740-3746.

- [26] Grebogi C., Ott E., Pelikan S., Yorke J.A. Strange attractors that are not chaotic // *Physica D*. 1984. Vol. 13. No. 1, 2. PP. 261-268.
- [27] Bezruchko B.P., Kuznetsov S.P., Seleznev Ye.P. Experimental observation of dynamics near the torus-doubling terminal critical point. // *Phys. Rev. E*. 2000. Vol. 62. No.6. PP.7828-7830.
- [28] Feudel U., Kuznetsov S., Pikovsky A. *Strange Nonchaotic Attractors. Dynamics between Order and Chaos in Quasiperiodically Forced Systems*. World Scientific: Singapore; 2006.
- [29] Kim S., Ostlund S. Simultaneous rational approximations in the study of dynamical systems // *Phys. Rev. A*. 1986. Vol. 34. No. 4. PP. 3426-3434.
- [30] Kuznetsov A.P., Kuznetsov S.P., Stankevich N.V. A simple autonomous quasiperiodic self-oscillator // *Communications in Nonlinear Science and Numerical Simulation*. 2010. Vol. 15. PP. 16761681.
- [31] Kuznetsov A.P., Kuznetsov S.P., Mosekilde E. and Stankevich N.V. Generators of quasiperiodic oscillations with three-dimensional phase space // *The European Physical Journal Special Topics*. 2013. Vol. 222. No. 10. PP. 2391-2398.
- [32] Kuznetsov A., Kuznetsov S., Seleznev E., Stankevich N. A generator of quasiperiodic oscillations: An autonomous dynamics and Synchronization of coupled generators // *Proceeding of NDES 2012*. P. 3.